Eur. Phys. J. D **31**, 45–51 (2004)
DOI: 10.1140/epjd/e2004-00134-y

THE EUROPEAN PHYSICAL JOURNAL D

Elastic and total cross-sections for electron scattering by acetylene in the intermediate energy range

I. Iga[1], M.-T. Lee[1], P. Rawat[1], L.M. Brescansin[2,a], and L.E. Machado[3]

[1] Departamento de Química, UFSCar, 13565-905 São Carlos, SP, Brazil
[2] Instituto de Física "Gleb Wataghin", UNICAMP, 13083-970 Campinas, SP, Brazil
[3] Departamento de Física, UFSCar, 13565-905 São Carlos, SP, Brazil

Received 7 June 2004 / Received in final form 26 August 2004
Published online 5 October 2004 –

Abstract. We present a joint theoretical-experimental study on electron scattering by C_2H_2 in the intermediate energy range. We report calculated elastic differential, integral, and momentum-transfer as well as total (elastic + inelastic) and absorption cross-sections at impact energies ranging from 10 to 500 eV. Also, experimental absolute elastic cross-sections are reported in the (50–500)-eV energy range. A complex optical potential is used to represent the electron-molecule interaction dynamics. The iterative Schwinger variational method, combined with the distorted-wave approximation, is used to solve the scattering equations. Experimentally, the angular distributions of the scattered electrons are converted to absolute cross-sections using the relative flow technique. The comparison of our calculated with our measured results, as well as with other experimental and theoretical data available in the literature, is encouraging.

PACS. 34.80.Bm Elastic scattering of electrons by atoms and molecules

1 Introduction

Electron scattering from small hydrocarbon molecules has been a subject of increasing interest, both theoretically and experimentally, in the past few years [1–12]. Electron-impact cross-sections for these molecules are important for understanding and modeling plasmas [13], to elucidate some mechanisms of astrophysical phenomena [14], and to control plasma processing in industry [15]. A critical review of experimental efforts on this matter was reported recently by Karwasz et al. [16]. Specifically for electron-acetylene collisions, some early experimental studies reported in the literature include measurements of relative grand total (elastic + inelastic) cross-sections (TCS) by Brüche [17] in the (1–40)-eV energy range and those of Dressler and Allan [18] in the (0.05–5)-eV energy range. Normalized and absolute TCS for e^-–C_2H_2 scattering were reported by Sueoka and Mori [19] in the (0.7–400)-eV energy range, by Xing et al. [20] between 400 and 2600 eV, and recently by Ariyasinghe and Powers [21] in the (200–1400)-eV energy range. A few experimental studies on elastic e^-–C_2H_2 scattering were also published over the years. In 1933, Hughes and McMillen [22] reported relative differential cross-sections (DCS) in the 10–150° angular range and (10–225)-eV energy range. Also, Fink et al. [23] reported relative DCS, normalized to the calculated results from the independent-atom model (IAM), in the 3–130° angular and (100–1000)-eV energy ranges. Absolute DCS at a single incident energy of 2 eV were reported by Kochem et al. [24]. More recently, absolute DCS obtained using the relative-flow technique (RFT) in the (5–100)-eV energy range were determined by Khakoo et al. [25]. Above 100 eV, there are no experimental results for absolute DCS for this target. In general, the DCS of Khakoo et al. agree in shape with the relative data of Hughes and McMillen, except at small scattering angles. In particular at 100 eV, as observed by Karwasz et al. [16], the DCS obtained by the three groups (Hughes and McMillen, Fink et al., and Khakoo et al.), normalized at 90° to the measured data of Khakoo et al., disagree with each other for scattering angles below 15°. Also, quantitatively, the DCS at 100 eV reported by Khakoo et al. and those of Fink et al. normalized to the IAM differ by a factor of two [16]. From the theoretical point of view, although numerous studies on e^-–C_2H_2 scattering have been reported over the past two decades, most of them were performed for incident energies below 100 eV. Cross-section calculations for electron scattering by this molecule above that energy are also scarce. In 1992, Jain and Baluja [26] calculated elastic integral cross-sections (ICS) as well as TCS for e^-–C_2H_2 in the (10–5000)-eV energy range using a complex optical potential approach. In their calculation, only the spherical part

[a] e-mail: bresca@ifi.unicamp.br

of the interaction potential was taken into account. More recently, TCS in the (10–1000)-eV were also calculated by Jiang et al. [3] using the additivity rule. DCS for elastic e^-–C_2H_2 scattering were calculated by Mu-Tao et al. [27] in the (10–200)-eV energy range, by Jain [28] in the (0–20)-eV energy range and by Gianturco and Stoecklin [29] in the (0–100)-eV energy range. The interaction potential used in Jain's calculation includes the exact static potential plus model exchange and polarization contributions, whereas an exact static-exchange potential plus a model polarization contribution is used in the calculations of Mu-Tao et al. and Gianturco and Stoecklin. In general, the DCS calculated by both Mu-Tao et al. [27] and Gianturco and Stoecklin [29] are larger than the absolute data of Khakoo et al. [25]. In principle, this discrepancy may be attributed either to errors in the experimental measurements or deficiencies of the calculations, e.g., the neglect of absorption effects. Such effects are known to be important at intermediate and high incident energies, where most inelastic channels (electronic excitations, ionization, etc.) are open, thus resulting in a reduction of the flux corresponding to the elastic channel. Those discrepancies clearly show the need of further experimental and theoretical investigations on elastic e^-–C_2H_2 collisions.

Recently, our group carried out a joint theoretical-experimental study on elastic e^-–C_2H_4 scattering [7] in the intermediate energy range. In that work, a complex optical potential, derived from a fully molecular near-Hartree-Fock self-consistent-field (SCF) wavefunction, is used to describe the electron-molecule interaction. The comparison between our calculated and experimental results, as well as with the existing data in the literature was encouraging. In this paper we extend such a joint study to the electron scattering by C_2H_2 in the intermediate energy range. Specifically, calculated DCS, ICS, momentum transfer cross-sections (MTCS), as well as TCS and total absorption cross-sections (TACS) are reported for incident energies ranging from 10 to 500 eV. Experimental absolute DCS, ICS, and MTCS in the (50–500)-eV energy range are also reported. In addition to providing reliable experimental cross-sections, it is hoped that the comparison of our measured data with those available in the literature at some common incident energies can help clarify the existent discrepancies among the experimental results [22,23,25], as well as to understand the role played by the absorption effects in the collisional dynamics.

The organization of this paper is as follows: in Section 2, the theory is briefly described and some details of the calculations are given, whereas some experimental details are briefly presented in Section 3. Finally, our calculated results are compared with the present experimental and other existing theoretical and/or experimental data in Section 4, where we also summarize our conclusions.

2 Theory and calculation

In the present study, a combination of the iterative Schwinger variational method (ISVM) and the distorted-wave approximation (DWA) is used to solve the scattering equations. Since the details of these methods have already been presented in previous works [30,31], they will be only briefly outlined here. The dynamics of e^--molecule scattering is described by a complex optical potential, given by:

$$V_{opt} = V_{st} + V_{ex} + V_{cp} + iV_{ab} \tag{1}$$

where V_{st} and V_{ex} are the static and the exchange components respectively, V_{cp} is the correlation-polarization contribution and V_{ab} is an absorption potential. In our calculation, V_{st} and V_{ex} are treated exactly, whereas V_{cp} is obtained in the framework of the free-electron-gas model, derived from a parameter-free local density, following the prescription of Padial and Norcross [32], where a short-range correlation potential between the scattering and the target electrons is defined in an inner region. The correlation potential is calculated by a free-electron-gas model, derived using the target electronic density according to equation (9) of Padial and Norcross [32]. In addition, an asymptotic form of the polarization potential is used for the long electron-target interaction. Experimental dipole polarizabilities $\alpha_0 = 22.473$ a.u. and $\alpha_2 = 11.972$ a.u. [33] were used to calculate the asymptotic form of V_{cp}. The absorption potential V_{ab} in equation (1) is taken as the semi-empirical version 3 of the quasi-free scattering model, derived by Staszewska et al. [34]. The implementation of these model potentials are discussed in references [6,10,11].

The scattering process is studied within the fixed-nuclei framework, where the DCS averaged over the molecular orientations are written as:

$$\frac{d\sigma}{d\Omega} = \frac{1}{8\pi^2}\int d\alpha \sin\beta d\beta d\gamma |f(\hat{k}'_0, \hat{k}')|^2, \tag{2}$$

where $f(\hat{k}'_0, \hat{k}')$ is the laboratory-frame scattering amplitude, $\hat{k}'_0$ and $\hat{k}'$ are the directions of incident- and scattered-electron linear momenta, respectively, and (α, β, γ) are the Euler angles which define the orientation of the principal axis of the molecule.

The quantity $f(\hat{k}'_0, \hat{k}')$ is related to the T-matrix elements by:

$$f(\hat{k}'_0, \hat{k}') = -2\pi^2 T. \tag{3}$$

Based on the two-potential formalism, the transition T matrix can be written as:

$$T_{fi} = \langle \Phi_f \mid U_1 \mid \chi_i^+ \rangle + \langle \chi_f^- \mid U_2 \mid \Psi_i^+ \rangle, \tag{4}$$

where the superscripts (+) and (−) designate the outgoing- and incoming-wave boundary conditions, respectively, and Ψ, χ, and Φ are solutions of the corresponding Schrödinger equations:

$$(H_0 + U - E)\Psi = 0, \tag{5}$$

$$(H_0 + U_1 - E)\chi = 0, \tag{6}$$

and

$$(H_0 - E)\Phi = 0, \tag{7}$$

where $H_0 = \nabla^2$ is the unperturbed Hamiltonian operator for a free electron and U is the total interaction potential that can be split arbitrarily as

$$U = U_1 + U_2. \tag{8}$$

In the present study, U_1 is taken as the real part of the optical potential, whereas U_2 is the imaginary absorption potential. The corresponding distorted-wave scattering equation (6) is solved using the ISVM [30]. Furthermore, the DWA is used to calculate the absorption part of the T matrix:

$$T_{ab} = i\langle \chi_f^- \mid V_{ab} \mid \chi_i^+ \rangle. \tag{9}$$

Moreover, the TCS for electron-molecule scattering are obtained using the optical theorem, viz.

$$\sigma_{tot} = \frac{4\pi}{k} \mathrm{Im}(f(\theta = 0^\circ)). \tag{10}$$

The SCF wavefunction for the ground state used in the static-exchange calculation was obtained using the contracted Gaussian basis set of reference [7]. It consists of the contracted set of Dunning [35] augmented with some uncontracted functions on the nuclei and on the center-of-mass of the molecule. At the experimental equilibrium geometry of $R_{(\mathrm{C-C})} = 2.2734$ a.u., $R_{(\mathrm{C-H})} = 2.003$ a.u., this basis set gives an SCF energy of –76.844741 a.u., in good agreement with the previous calculated value of −76.831406 a.u. [27].

In ISVM calculations, the target and the scattering wavefunctions, as well as the interaction potentials and all calculated matrices are partial-wave expanded about the center-of-mass of the molecule. The truncation parameters used in these expansions are: $l_c = 28$ for the bound orbitals, $l_c = 50$ for V_{st}, $l_c = 20$ for both V_{ex} and V_{ab}. The scattering wavefunctions and the T_{ab} matrix elements are truncated at $l_c = 40$ and $m_c = 17$. With these parameters, the resulting normalizations of the bound orbitals are better than 0.999. All our ISVM results are converged within two iterations.

3 Experiment

Details of our experimental set-up and procedure have already been presented in previous works [10,36] and will only be briefly described here. A crossed electron beam-molecular beam geometry is used to measure the relative distribution of the scattered electrons as a function of the scattering angle at a given incident energy. The scattered electrons are energy-filtered by a retarding-field energy selector with a resolution of about 1.5 eV. This resolution is sufficient to distinguish electronically inelastic scattered electrons; however it cannot resolve vibrational levels. Thus, our measured DCS are indeed vibrationally summed. During the measurements, the working pressure in the vacuum chamber is around 5×10^{-7} torr. The recorded scattering intensities are converted into absolute elastic DCS using the well known RFT [37,38], in which Ar is used as the secondary standard. The e^-−Ar absolute cross-sections of Jansen et al. [39] in the (100–500)-eV energy range and Panajotovic et al. [40] for 50 and 80 eV are used to normalize our data. Details of the analysis on experimental uncertainties have also been given elsewhere [10]. They are estimated briefly as follows. Uncertainties of random nature such as pressure fluctuations, electron beam current readings, background scattering, etc., are estimated to be less than 2%. These contributions, combined with the estimated statistical errors, give an overall uncertainty of 4% in the relative DCS for each gas. Also, the experimental uncertainty associated with the normalization procedure is estimated to be 5.7%. These errors, combined with the quoted ones [39,40] in the absolute DCS of the secondary standard, provide an overall experimental uncertainty of 11% in our absolute DCS. The absolute DCS were determined in the 8–130° angular range. In order to obtain the ICS and MTCS, an extrapolation procedure was adopted to estimate the DCS at scattering angles out of that angular range. The extrapolation was carried out following the trend of the theoretical DCS in both forward and backward directions. The overall errors on ICS and MTCS are estimated to be 22%.

4 Results and discussion

The present experimental data of DCS, ICS, and MTCS, measured in the (50–500)-eV energy range, are presented in Table 1.

In Figures 1–3 we compare our calculated DCS with our experimental values and the absolute data of Khakoo et al. [25], and with the calculated results of Mu-Tao et al. [27], Jain [28], and Gianturco and Stoecklin [29] at some common incident energies. The relative DCS of Fink et al. [23] at incident energies $E_0 = 100$ and 200 eV, normalized to our absolute values at the scattering angle of 40°, are also shown for comparison. At 10 eV, where only a few inelastic channels are open, the DCS obtained from three different calculations (the present, Jain [28], and Gianturco and Stoecklin [29]) agree well with each other (see Fig. 1a). Also at this energy, the agreement between these theoretical results and the experimental data of Khakoo et al. is fairly good. On the other hand, the calculation of Mu-Tao et al. [27] strongly overestimates the DCS at small scattering angles, probably due to the use of a very crude model polarization potential adopted in that study. At higher incident energies, the discrepancies between our calculated DCS and those of Mu-Tao et al. and of Gianturco and Stoecklin become evident. In particular, the calculated results of the latter two papers lie well above our data in the intermediate and large angular ranges. This overestimation is attributed to the neglect of the absorption effects in those works. In order to better illustrate the influence of these effects, we present the DCS calculated without the inclusion of the absorption potential for incident energies of 300 and 500 eV. Also at these energies, the neglect of absorption effects leads to the overestimation of DCS as can be seen in Figure 3.

Table 1. Experimental DCS, ICS and MTCS (in 10^{-16} cm^2) for elastic e^-–C_2H_2 scattering.

Angle		E_0 (eV)		
(deg)	50	80	100	150
8	2.23(1)*	2.06(1)	1.97(1)	1.55(1)
10	1.87(1)	1.60(1)	1.19(1)	9.59(0)
15	1.06(1)	8.08(0)	6.01(0)	4.90(0)
20	5.51(0)	4.00(0)	2.86(0)	2.02(0)
30	1.67(0)	1.07(0)	7.70(–1)	5.52(–1)
40	6.18(–1)	3.93(–1)	2.90(–1)	2.66(–1)
50	2.77(–1)	1.94(–1)	1.80(–1)	1.75(–1)
60	1.65(–1)	1.43(–1)	1.24(–1)	1.15(–1)
70	1.42(–1)	1.04(–1)	8.46(–2)	7.85(–2)
80	1.06(–1)	7.98(–2)	6.81(–2)	5.98(–2)
90	1.07(–1)	7.82(–2)	6.98(–2)	5.01(–2)
100	1.21(–1)	8.00(–2)	6.84(–2)	5.35(–2)
110	1.60(–1)	9.66(–2)	7.15(–2)	5.29(–2)
120	2.29(–1)	1.09(–1)	8.73(–2)	6.12(–2)
130	3.00(–1)	1.42(–1)	1.01(–1)	6.88(–2)
ICS	9.92(0)	7.43(0)	6.01(0)	4.72(0)
MTCS	3.46(0)	1.92(0)	1.44(0)	1.02(0)
Angle		E_0 (eV)		
(deg)	200	300	400	500
8	1.28(1)	1.09(1)	8.26(0)	6.41(0)
10	8.45(0)	6.92(0)	4.83(0)	3.86(0)
15	3.41(0)	2.74(0)	1.85(0)	1.27(0)
20	1.55(0)	1.14(0)	7.37(–1)	6.07(–1)
30	4.14(–1)	3.94(–1)	3.21(–1)	2.88(–1)
40	2.35(–1)	2.34(–1)	1.42(–1)	1.03(–1)
50	1.51(–1)	1.14(–1)	6.31(–2)	4.97(–2)
60	8.15(–2)	6.02(–2)	3.84(–2)	3.36(–2)
70	5.42(–2)	4.41(–2)	2.53(–2)	2.01(–2)
80	3.97(–2)	3.59(–2)	1.77(–2)	1.31(–2)
90	3.64(–2)	2.88(–2)	1.26(–2)	1.06(–2)
100	3.36(–2)	2.12(–2)	1.17(–2)	8.70(–3)
110	3.29(–2)	1.98(–2)	9.10(–3)	7.40(–3)
120	3.29(–2)	2.00(–2)	8.20(–3)	6.20(–3)
130	3.31(–2)	2.00(–2)	7.20(–3)	6.00(–3)
ICS	3.78(0)	3.17(0)	2.33(0)	1.81(0)
MTCS	6.17(–1)	4.43(–1)	2.37(–1)	1.88(–1)

*2.23(1) means 2.23×10^1.

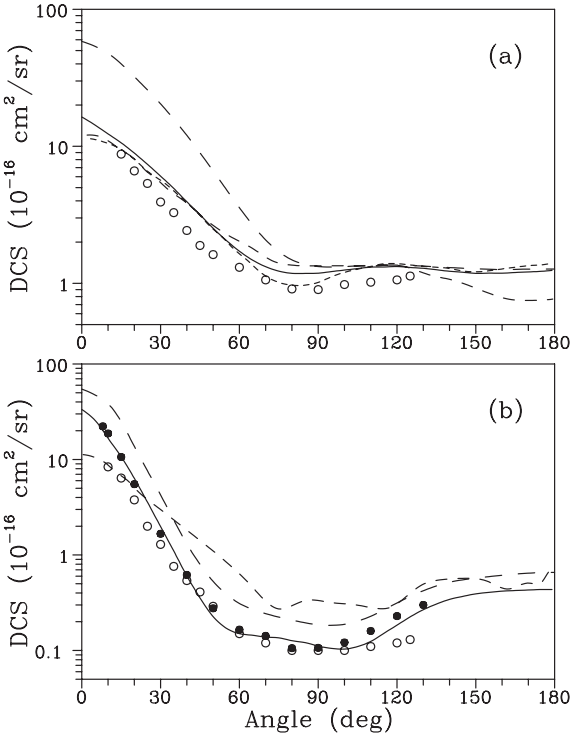

Fig. 1. DCS for elastic e^-–C_2H_2 scattering at incident energies of (a) 10 eV, and (b) 50 eV. Solid line, present calculated results; short-dashed line, calculated results of Jain [28]; dashed line, calculated results of Gianturco and Stoecklin [29]; long-dashed line, theoretical results of Mu-Tao et al. [27]; open circles, experimental results of Khakoo et al. [25]; full circles, present experimental results.

The present calculated results accounting for the absorption effects are in better agreement with the experimental DCS, both in shape and magnitude, particularly for energies above 100 eV.

On the other hand, our experimental results and the previous measured data of Khakoo et al. at 50 and 100 eV show different angular behaviors. There is a good agreement at intermediate scattering angles (30–100°); however, the present measured DCS are larger than theirs out of this angular range. In addition, an excellent agreement is seen between our experimental data and the normalized DCS of Fink et al. at 100 and 200 eV, in the entire angular range.

In Figures 4a and 4b we compare our calculated ICS and MTCS in the (10–500)-eV energy range with the present experimental data and the experimental ICS of Khakoo et al. [25]. The calculated ICS and MTCS of Jain [28], the calculated ICS of Mu-Tao et al. [27] and of Jain and Baluja [26], as well as the calculated MTCS of Gianturco and Stoecklin [29] are also shown for comparison. There is a very good agreement between our calculated and our measured data. The calculated results of Jain and of Gianturco and Stoecklin also agree quite well with our theoretical results at low incident energies, whereas the calculated ICS of Mu-Tao et al. and of Jain and Baluja are larger than ours in the entire energy range. On the other hand, the experimental ICS of Khakoo et al. lie 30% to 40% below our measured data. These discrepancies are probably originated by the underestimation of their DCS at small scattering angles and also by the extrapolation procedure towards the forward direction. The DCS for small scattering angles contribute significantly to the ICS.

Figure 5a presents our calculated TCS in the (10–500)-eV energy range along with the experimental data of Sueoka and Mori [19] and Ariyasinghe and Powers [21], as well as the calculated results of Jain and

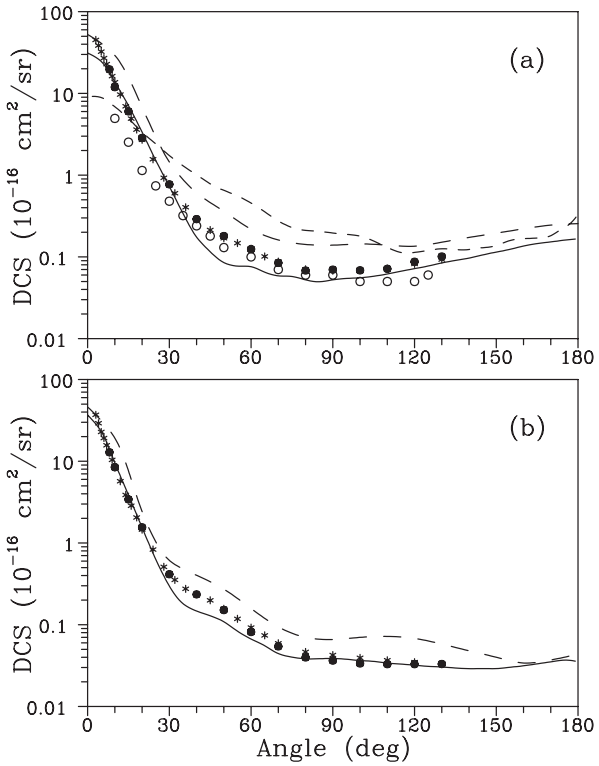

Fig. 2. The same as Figure 1, but for (a) 100 eV and (b) 200 eV. The symbols are the same as in Figure 1, except: asterisks, relative DCS of Fink et al. [23], normalized to our experimental data at 40°.

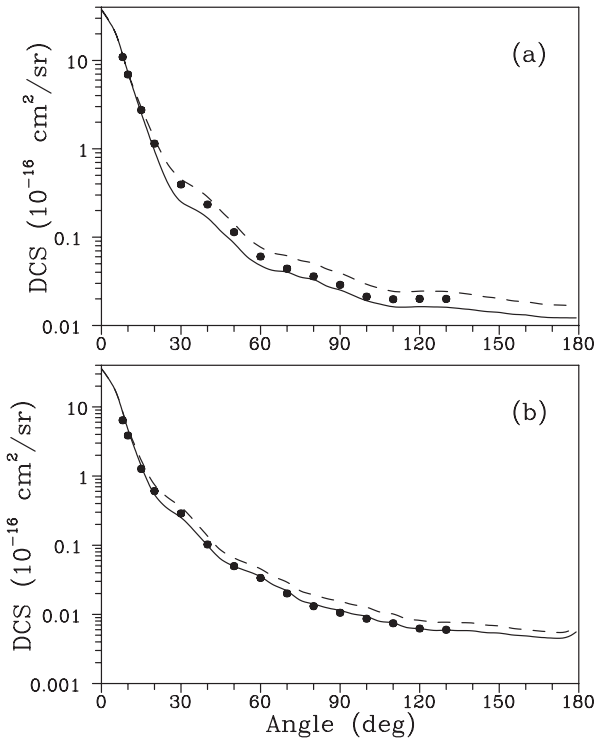

Fig. 3. The same as Figure 2, but for (a) 300 eV and (b) 500 eV. Dashed-line, present calculated results without the absorption effects.

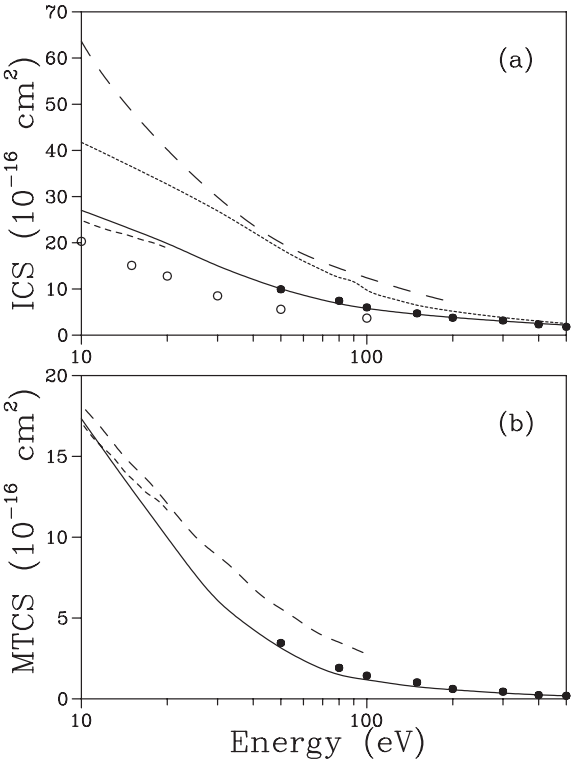

Fig. 4. (a) ICS and (b) MTCS, for elastic e^-–C_2H_2 scattering. The symbols are the same as in Figures 1 and 2, except: dotted line, calculated results of Jain and Baluja [26].

Baluja [26] and of Jiang et al. [3]. While the present study is unable to provide directly the electron-impact total ionization cross-sections (TICS) for e^-–C_2H_2, the difference between the calculated TCS and ICS provides an estimate of the TACS, which account for all inelastic contributions including both excitation and ionization processes. Nevertheless, Joshipura et al. [41] have observed that for a set of molecules, ionization dominates the inelastic processes, the values of the TICS being about 80% of the TACS at energies around 100 eV and about 100% for energies above 300 eV. Therefore, the comparison of the present calculated TACS with experimental and calculated TICS is meaningful and would provide insights of the electron-impact ionization dynamics of this molecule. They are shown in Figure 5b along with the measured TICS of Gaudin and Hagemann [42], Tian and Vidal [43], and Zheng and Srivastava [44], and also with the calculated TICS of Kim et al. [45] using the binary-encounter Bethe (BEB) model and the TACS of Jain and Baluja [26].

In general, our calculated TCS are in good agreement with all experimental data for incident energies of 50 eV and above. At lower energies, our results are at most 20% larger than those of Sueoka and Mori [19], which is still quite reasonable. The calculations of Jain and Baluja [26] and of Jiang et al. [3] overestimate the TCS. In addition, the present calculated TACS agree fairly well with the experimental TICS of Tian and Vidal [43], and Zheng and Srivastava [44] in the (15–50)-eV energy range. A general

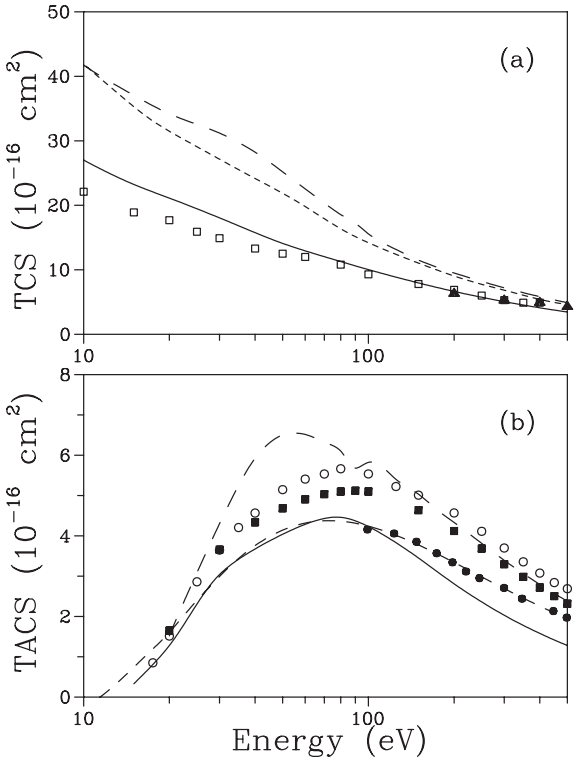

Fig. 5. (a) TCS, and (b) TACS for e^-–C_2H_2 scattering. Solid line, present calculated data; long-dashed line, calculated results of Jain and Baluja [26]; short-dashed line, calculated results of Jiang et al. [3]; open squares, measured TCS of Sueoka and Mori [19]; full triangles, experimental TCS of Ariyasinghe and Powers [21]; full circles, experimental TICS of Gaudin and Hagemann [42]; open circles, experimental TICS of Tian and Vidal [43]; full squares, experimental TICS of Zheng and Srivastava [44]; dashed-line, BEB TICS of Kim et al. [45].

good agreement is also seen between the calculated TICS of Kim et al. [45] and our TACS. At higher incident energies, our calculated data also agree reasonably well with those of Gaudin and Hagemann [42]. However, they lie systematically below the experimental TICS of Tian and Vidal [43], and of Zheng and Srivastava [44], as well as below the calculated TACS of Jain and Baluja [26].

In summary, we performed a joint theoretical-experimental study on e^-–C_2H_2 scattering in the intermediate energy range. A new set of absolute DCS, ICS, and MTCS in the (50–500)-eV energy range is presented. To our knowledge, the absolute data above 100 eV are published here for the first time. The comparison of the present measured DCS with the absolute data of Khakoo et al. [25] and with the normalized results of Fink et al. [23] shows a possible underestimation of the DCS of Khakoo et al. near the forward and backward directions. As a consequence of this underestimation, their ICS lie about 30% to 40% below our data. In addition, the good agreement seen between the present calculated and experimental cross-sections in the (50-500)-eV energy range has confirmed the relevant influence of absorption effects. Although such a simple model potential is able to provide accurate elastic DCS, ICS, and MTCS, the used model absorption potential may need some improvement in order to adequately describe quantitative TACS.

This research was partially supported by the Brazilian agencies CNPq and FAPESP.

References

1. C. Winstead, P.G. Hipes, M.A.P. Lima, V. Mckoy, J. Chem. Phys. **94**, 5455 (1991)
2. M.H.F. Bettega, A.P.P. Natalense, M.A.P. Lima, L.G. Ferreira, J. Chem. Phys. **103**, 10566 (1995)
3. Y. Jiang, J. Sun, L. Wan, Z. Phys. D **34**, 29 (1995)
4. F.A. Gianturco, J.A. Rodrigues-Ruiz, N. Sanna, J. Phys. B: At. Mol. Opt. Phys. **28**, 1287 (1995)
5. M.H.F. Bettega, A.J.S. Oliveira, A.P.P. Natalense, M.A.P. Lima, L.G. Ferreira, Eur. Phys. J. D **1**, 291 (1998)
6. L.E. Machado, M.-T. Lee, L.M. Brescansin, Braz. J. Phys. **28**, 111 (1998)
7. L.M. Brescansin, P. Rawat, I. Iga, M.G.P. Homem, M.-T. Lee, L.E. Machado, J. Phys. B: At. Mol. Opt. Phys. **37**, 471 (2004)
8. L. Boesten, H. Tanaka, J. Phys. B **24**, 821 (1991)
9. I. Kanik, S. Trajmar, J.C. Nickel, J. Geophys. Res. **98**, 7447 (1993)
10. I. Iga, M.-T. Lee, M.G.P. Homem, L.E. Machado, L.M. Brescansin, Phys. Rev. A **61**, 227081 (2000)
11. M.-T. Lee, I. Iga, L.E. Machado, L.M. Brescansin, Phys. Rev. A **62**, 062710 (2000)
12. R. Panajotovic, M. Kitajima, H. Tanaka, M. Jelisavcic, J. Lower, L. Campbell, M.J. Brunger, S.J. Buckman, J. Phys. B: At. Mol. Opt. Phys. **36**, 1615 (2003)
13. R.K. Janev, in *Atomic and Plasma-Material Interaction Processes in Controlled Thermonuclear Fusion*, edited by R.K. Janev, H.W. Drawin (Elsevier, Amsterdam, 1993), p. 27.
14. J.J. Perry, Y.H. Kim, J.L. Fox, H.S. Porter, J. Geophys. Res. **104**, 16541 (1999)
15. W.L. Morgan, Adv. At. Mol. Opt. Phys. **43**, 79 (2000)
16. P.G. Karwasz, R.S. Brusa, A. Zecca, Riv. Nuovo Cim. **24**, 1 (2001)
17. E. Brüche, Ann. Phys. (Leipzig) **2**, 909 (1929)
18. R. Dressler, M. Allan, J. Chem. Phys. **87**, 4510 (1987)
19. O. Sueoka, S. Mori, J. Phys. B: At. Mol. Opt. Phys. **22**, 963 (1989)
20. S.L. Xing, Q.C. Shi, X.J. Chen, K.Z. Xu, B.X. Yang, S.L. Wu, R.F. Feng, Phys. Rev. A **51**, 414 (1995)
21. W.M. Ariyasinghe, D. Powers, Phys. Rev. A **66**, 052716 (2002)
22. A.L. Hughes, J.H. McMillen, Phys. Rev. **44**, 876 (1933)
23. M. Fink, K. Jost, D. Herrmann, J. Chem. Phys. **63**, 1985 (1975)
24. K.-H. Kochem, E. Sohn, H. Ehrhardt, E.S. Chang, J. Phys. B: At. Mol. Opt. Phys. **18**, 1253 (1985)
25. M.A. Khakoo, T. Jayaweera, S. Wang, S. Trajmar, J. Phys. B: At. Mol. Opt. Phys. **26**, 4845 (1993)
26. A. Jain, K.L. Baluja, Phys. Rev. A **45**, 202 (1992)
27. L. Mu-Tao, L.M. Brescansin, M.A.P. Lima, L.E. Machado, E. Leal, J. Phys. B: At. Mol. Opt. Phys. **23**, 4331 (1990)

28. A. Jain, J. Phys. B: At. Mol. Opt. Phys. **26**, 4833 (1993)
29. F.A. Gianturco, T. Stoecklin, J. Phys. B: At. Mol. Opt. Phys. **27**, 5903 (1994)
30. R.R. Lucchese, G. Raseev, V. McKoy, Phys. Rev. A **25**, 2572 (1982)
31. M.-T. Lee, V. McKoy, Phys. Rev. A **28**, 697 (1983)
32. N.T. Padial, D.W. Norcross, Phys. Rev. A **29**, 1742 (1984)
33. J.O. Hirschfelder, C.F. Curtis, R.B. Bird, *Molecular Theory of Gases and Liquids* (John Wiley Sons, New York, 1954)
34. G. Staszewska, D.W. Schwenke, D.W. Truhlar, Phys. Rev. A **29**, 3078 (1984)
35. T.H. Dunning Jr, J. Chem. Phys. **53**, 2823 (1970)
36. P. Rawat, I. Iga, M.-T. Lee, L.M. Brescansin, L.E. Machado, M.G.P. Homem, Phys. Rev. A **68**, 052711 (2003)
37. S.K. Srivastava, A. Chutjian, S. Trajmar, J. Chem. Phys. **63**, 2659 (1975)
38. J.C. Nickel, P.W. Zetner, G. Shen, S. Trajmar, J. Phys. E **22**, 730 (1989)
39. R.H.J. Jansen, F.J. de Heer, H.J. Luyken, B. van Wingerden, H.J.B. Laauw, J. Phys. B: At. Mol. Opt. Phys. **9**, 185 (1976)
40. R. Panajotovic, D. Filipovic, B. Marinkovic, V. Pejcev, M. Kurepa, L. Vuskovic, J. Phys. B: At. Mol. Opt. Phys. **30**, 5877 (1997)
41. K.N. Joshipura, M. Vinodkumar, U. Patel, J. Phys. B: At. Mol. Opt. Phys. **34**, 509 (2001)
42. A. Gaudin, R. Hagemann, J. Chem. Phys. **64**, 1209 (1967)
43. C. Tian, C.R. Vidal, J. Phys. B: At. Mol. Opt. Phys. **31**, 895 (1998)
44. S.-H. Zheng, S.K. Srivastava, J. Phys. B: At. Mol. Opt. Phys. **29**, 3235 (1996)
45. Y.-K. Kim, M.A. Ali, M.E. Rudd, J. Res. NIST A **102**, 692 (1997)